JB
Journals.ASM.org

Hydrogen Formation and Its Regulation in *Ruminococcus albus*: Involvement of an Electron-Bifurcating [FeFe]-Hydrogenase, of a Non-Electron-Bifurcating [FeFe]-Hydrogenase, and of a Putative Hydrogen-Sensing [FeFe]-Hydrogenase

Yanning Zheng,[a] Jörg Kahnt,[a] In Hyuk Kwon,[b] Roderick I. Mackie,[b] Rudolf K. Thauer[a]

Max Planck Institute for Terrestrial Microbiology, Marburg, Germany[a]; Department of Animal Sciences, Institute for Genomic Biology, University of Illinois at Urbana-Champaign, Urbana, Illinois, USA[b]

Ruminococcus albus* 7 has played a key role in the development of the concept of interspecies hydrogen transfer. The rumen bacterium ferments glucose to 1.3 acetate, 0.7 ethanol, 2 CO_2, and 2.6 H_2 when growing in batch culture and to 2 acetate, 2 CO_2, and 4 H_2 when growing in continuous culture in syntrophic association with H_2-consuming microorganisms that keep the H_2 partial pressure low. The organism uses NAD^+ and ferredoxin for glucose oxidation to acetyl coenzyme A (acetyl-CoA) and CO_2, NADH for the reduction of acetyl-CoA to ethanol, and NADH and reduced ferredoxin for the reduction of protons to H_2. Of all the enzymes involved, only the enzyme catalyzing the formation of H_2 from NADH remained unknown. Here, we report that *R. albus* 7 grown in batch culture on glucose contained, besides a ferredoxin-dependent [FeFe]-hydrogenase (HydA2), a ferredoxin- and NAD-dependent electron-bifurcating [FeFe]-hydrogenase (HydABC) that couples the endergonic formation of H_2 from NADH to the exergonic formation of H_2 from reduced ferredoxin. Interestingly, *hydA2* is adjacent to the *hydS* gene, which is predicted to encode an [FeFe]-hydrogenase with a C-terminal PAS domain. We showed that *hydS* and *hydA2* are part of a larger transcriptional unit also harboring putative genes for a bifunctional acetaldehyde/ethanol dehydrogenase (Aad), serine/threonine protein kinase, serine/threonine protein phosphatase, and a redox-sensing transcriptional repressor. Since HydA2 and Aad are required only when *R. albus* grows at high H_2 partial pressures, HydS could be a H_2-sensing [FeFe]-hydrogenase involved in the regulation of their biosynthesis.

The genus *Ruminococcus* (class *Clostridia*) consists of species of anaerobic, Gram-positive bacteria. One or more species of this genus are found in significant numbers in the intestines of humans (enterotype 3) (1, 2) and in the rumen and colon of herbivores (3, 4). *Ruminococcus flavefaciens* and *Ruminococcus albus* are among the most important plant cell wall-degrading bacteria in the rumen. These two species produce all required enzymes for hydrolyzing the plant cell wall polysaccharides, cellulose and hemicellulose (5, 6).

R. albus was isolated in 1957 from the rumen of cattle by Hungate (7, 8), who showed that in batch culture the bacterium ferments cellulose, cellobiose, or glucose to acetate, CO_2, ethanol, and H_2. Nevertheless, neither H_2 nor ethanol accumulate to high concentrations in the rumen (9, 10). The low H_2 concentrations in the rumen have been explained by the presence of H_2-consuming microorganisms, such as *Methanobrevibacter ruminantium* (formerly *Methanobacterium ruminantium*), that consume H_2 more rapidly than it is formed from cellulose by *R. albus* (11). The laboratory of Bryant and Wolin then showed in 1973 that the fermentation of glucose by *R. albus* strain 7 was shifted from 1.3 acetic acid, 0.7 ethanol, 2 CO_2, and 2.6 H_2 in batch culture to 2 acetic acid, 2 CO_2, and 4 H_2 in chemostat culture together with *Wolinella succinogenes* (formerly *Vibrio succinogenes*), which grew on H_2 and fumarate producing succinate, keeping the H_2 concentration low (12). The interspecies cooperation allowed *W. succinogenes* to grow at the expense of H_2 produced by *R. albus*, but it also offered an energetic advantage to *R. albus* in the form of a higher ATP gain (4 mol of ATP instead of 3.3 mol of glucose fermented) and, consequently, a better growth yield (13). At low H_2 partial pressures, the free energy associated with glucose fermentation is more negative than that at high H_2 partial pressures, which is the thermodynamic basis for the different ATP gains (13). The fermentation of *R. albus* on glucose has been modeled (14). The literature on interspecies H_2 and formate transfer has been reviewed recently (15).

Enzymatic analyses have revealed that *R. albus* strain 7 grown in batch culture on glucose contains an NAD-specific glyceraldehyde-3-phosphate dehydrogenase, a pyruvate:ferredoxin oxidoreductase, a ferredoxin (Fd)-dependent hydrogenase, an NAD-specific acetaldehyde dehydrogenase (coenzyme A [CoA] acetylating), and an NAD-specific ethanol dehydrogenase. These enzymes are present in the cell extract of *R. albus* at specific activities sufficient to account for the observed fermentation rates (16). In the fermentation, more H_2 is formed (2.6 mol) than pyruvate is oxidized (2 mol). To account for this difference, an unidentified NADH:ferredoxin oxidoreductase in *R. albus* must catalyze the reduction of Fd with NADH (13) (see Fig. S1 in the supplemental material). Such an activity was indeed found but at a specific ac-

Received 8 July 2014 **Accepted** 21 August 2014
Published ahead of print 25 August 2014
Address correspondence to Rudolf K. Thauer, thauer@mpi-marburg.mpg.de.
Supplemental material for this article may be found at http://dx.doi.org/10.1128/JB.02070-14.

doi:10.1128/JB.02070-14

tivity that was much too low to account for the observed fermentation rates (16). In addition, it was difficult to envisage thermodynamically how NADH with a redox potential, E′, *in vivo* that was more positive than −320 mV (13, 17) could provide the electrons for hydrogen formation from protons at a redox potential that was more negative than −400 mV considering that H_2 can be observed bubbling out of the medium when *R. albus* grows at pH 7 in the absence of a H_2-consuming partner. The E_0' of the 2×[4Fe4S] ferredoxin from *R. albus* is −420 mV (18, 19). *In vivo*, the E′ of the ferredoxin is probably near the E_0' of the acetyl-CoA + CO_2/pyruvate couple, which is −500 mV (20).

A solution to this problem was recently shown for *Thermotoga maritima* growing fermentatively at 80°C in batch culture on glucose, which, at this temperature, is fermented to 2 acetic acid, 2 CO_2, and 4 H_2 and involves the same enzymes as those in *R. albus*. The bacterium contains a ferredoxin- and NAD-dependent electron-bifurcating [FeFe]-hydrogenase (HydABC) that couples the endergonic reduction of protons with NADH to H_2 to the exergonic reduction of protons with reduced ferredoxin to H_2 (21, 22) in the reaction NADH + Fd_{red}^{2-} + 3 H^+ ⇄ NAD^+ + Fd_{ox} + 2 H_2, where Fd_{red} is reduced ferredoxin and Fd_{ox} is oxidized ferredoxin.

The electron-bifurcating hydrogenase subsequently was found in *Acetobacterium woodii* (23) and *Moorella thermoacetica* (24, 25), in which the enzyme catalyzes the reduction of ferredoxin and NAD^+ with H_2 when these acetogens grow on H_2 and CO_2. In *Clostridium autoethanogenum*, an NADP-specific electron-bifurcating [FeFe]-hydrogenase is present (26).

In the meantime, a closed sequence of the genome of *R. albus* strain 7 has been obtained (27). The draft genomes of *R. albus* strains 8 and SY3 also are available (http://www.ncbi.nlm.nih.gov/genome/genomes/1019). Strain 7 contains a 3,685,408-bp circular chromosome and four circular plasmids: pRumal01 (420,706 bp), pRumal02 (352,646 bp), pRumal03 (15,907 bp), and pRumal04 (7,420 bp). Only one set of chromosomal genes, encoding one hydrogenase, have been identified, namely, the genes *hydABC*, encoding a putative electron-bifurcating [FeFe]-hydrogenase. The gene for a second [FeFe]-hydrogenase is found on plasmid pRumal01. It is predicted to code for a monomeric, ferredoxin-dependent [FeFe]-hydrogenase (HydA2) with 27% sequence identity to HydA of the putative electron-bifurcating [FeFe]-hydrogenase. Both HydA and HydA2 from *R. albus* are predicted to harbor the active-site [FeFe]-[4Fe4S] center (H-cluster) (28, 29), three [4Fe4S]-clusters, and one [2Fe2S]-cluster. The genes *hydE*, *hydF*, and *hydG* for [FeFe]-hydrogenase maturation (28) are chromosomal but are not adjacent to *hydABC*.

On plasmid pRumal01, adjacent to *hydA2*, lies a gene tentatively annotated *hydS* (S for signaling). It is predicted to encode a protein with a noncanonical H-cluster, three [4Fe4S]-clusters, and a C-terminal PAS domain. PAS domains have important sensory functions within sensory proteins, are widely utilized in all three domains of life, and consist of ca. 100 amino acids. They promote protein-protein interaction or signal transfer and perceive environmental cues either directly, e.g., the concentration of dicarboxylic acids, or indirectly via a prosthetic group, e.g., the concentration of dissolved gases, redox potential, or visible light (30). Proteins containing a PAS domain in addition to an [FeFe]-hydrogenase domain have been noted in genome sequences of several anaerobic bacteria, including *Carboxydothermus hydrogenoformans* (31), *Halothermothrix orenii* (32), *Treponema* species (33), and *Thermoanaerobacterium saccharolyticum* (34). The PAS domain in the [FeFe]-hydrogenase HfsB of *T. saccharolyticum* appears to have a regulatory role, as the deletion of the *hfsABCD* genes negatively affected transcription of the *hydABC* genes encoding a heterotrimeric [FeFe]-hydrogenase (35).

Here, we show that cells of *R. albus* 7 grown in batch culture on glucose contain an electron-bifurcating ferredoxin- and NAD-dependent [FeFe]-hydrogenase and a ferredoxin-dependent [FeFe]-hydrogenase encoded by the genes *hydABC* and *hydA2*, respectively. We also show that the gene *hydS*, which encodes the putative H_2-sensing [FeFe]-hydrogenase, forms a transcriptional unit together with *hydA2* and putative genes for a redox-sensing transcriptional repressor, a bifunctional acetaldehyde/ethanol dehydrogenase, a serine/threonine protein kinase, and a serine/threonine protein phosphatase.

MATERIALS AND METHODS

Chemicals, enzymes, and organisms. NAD^+, $NADP^+$, NADH, NADPH, flavin adenine dinucleotide (FAD), flavin mononucleotide (FMN), thiamine pyrophosphate, coenzyme A, pyruvate, glyceraldehyde phosphate, 3-phosphoglyceric acid (disodium salt), acetyl-phosphate (lithium potassium salt), acetaldehyde, methyl viologen, dithiothreitol (DTT), 3-phosphoglycerate kinase, and phosphotransacetylase were from Sigma-Aldrich Chemie GmbH (Taufkirchen, Germany). Galactose and galactose dehydrogenase were from Merck (Darmstadt, Germany) and Roche (Mannheim, Germany), respectively. Oxidized ferredoxin (ε_{390} = 30.6 mM^{-1} cm^{-1}) (36) was purified from *Clostridium pasteurianum* (37), and pyruvate:ferredoxin oxidoreductase was purified from *R. albus* 7 as described below. H_2, N_2, and CO (99.996%) were from Messer (Düsseldorf, Germany). *R. albus* strain 7 (DSM 20455), *C. pasteurianum* (DSM 525), and *M. thermoacetica* (DSM 521) were from the Deutsche Sammlung von Mikroorganismen und Zellkulturen GmbH, Braunschweig, Germany.

Growth of bacteria. *R. albus* 7 was grown strictly anaerobically at 37°C in 2-liter glass bottles containing 1 liter of medium and 1 liter of N_2 as the gas phase. The bottles were closed with rubber stoppers, and overpressure was removed once in the middle of the fermentation. A slightly modified DSMZ 436 medium was used containing 0.5% glucose rather than 0.2% cellobiose and 0.3% glucose. Other components of the 1-liter medium were tryptone (0.5%); yeast extract (0.2%); 40 ml 0.6% K_2HPO_4; 40 ml solution containing 0.6% KH_2PO_4, 2% $(NH_4)_2SO_4$, 1.2% NaCl, 0.25% $MgSO_4 \cdot 7H_2O$, and 0.16% $CaCl_2 \cdot 2H_2O$; Na_2CO_3 (0.4%); cysteine-HCl · H_2O (0.05%); 1 ml volatile fatty acid mixture (10 ml isovaleric acid, 10 ml isobutyric acid, 10 ml 2-methylbutyric acid, 10 ml valeric acid, and 60 ml distilled water; adjusted to pH 7 with solid KOH); and resazurin (1 mg). $FeSO_4 \cdot 7H_2O$ (12.3 mg/liter) was added after autoclaving. Eighty milliliters of an exponentially growing culture (doubling time of approximately 2 h) at an optical density at 600 nm (OD_{600}) of 1.2 to 1.5 was used as the inoculum. After 16 h of incubation, when the cultures had reached an OD_{600} of around 2, the cells were harvested in an anaerobic chamber by centrifugation at 8,000 × *g* for 20 min. The harvested cells (4 g wet mass per liter of culture) were stored at −80°C under 95% N_2 and 5% H_2.

For the preparation of ferredoxin, *C. pasteurianum* was grown in glucose-ammonium medium to an OD_{600} of 7 to 8 (38). For the preparation of cell extract containing carbon monoxide dehydrogenase, *M. thermoacetica* was grown on glucose medium to an OD_{660} of 5 (24).

Preparation of cell extracts. Frozen cells of *R. albus* 7 were suspended in a 2-fold volume (wt/vol) of anoxic 50 mM Tris-HCl (pH 7.6) containing 2 mM DTT, 10 μM FAD, and 10 μM FMN. After adding DNase I (1 mg/4 g wet cell), the cell suspension was passed through a prechilled French pressure cell twice at 120 MPa. Before this step, the French pressure cell initially was flushed with N_2 for 5 min and then washed twice with anoxic buffer. Unbroken cells and cell debris were removed by centrifugation at 10,000 × *g* at 4°C for 30 min. The supernatant was used for enzyme assays. For protein purification, the supernatant was further cen-

trifuged at 150,000 × *g* at 4°C for 60 min to remove the membrane proteins (25).

Determination of specific activities. Enzyme activities were measured under strictly anoxic conditions at 37°C in 1.5-ml anoxic cuvettes or, when H_2 formation was to be determined, in 6.5-ml anoxic serum bottles sealed with rubber stoppers. After the start of the reaction with cell extract or purified enzyme, the reduction of $NAD(P)^+$ was monitored photometrically at 340 nm ($\varepsilon = 6.2\ mM^{-1}\ cm^{-1}$) (39), reduction of ferredoxin at 430 nm ($\Delta\varepsilon_{ox\text{-}red} \approx 13.1\ mM^{-1}\ cm^{-1}$) (36, 40), and reduction of methyl viologen at 578 nm ($\varepsilon = 11.1\ mM^{-1}\ cm^{-1}$) (41, 42). The formation of H_2 was monitored using gas chromatography (25). The serum bottles were continuously shaken at 200 rpm to ensure H_2 transfer from the liquid phase into the gas phase. Gas samples (0.1 ml) were withdrawn every 2 min.

Proteins were quantified using the Bio-Rad protein assay (Munich, Germany) with bovine serum albumin as the standard.

Glyceraldehyde-3-phosphate dehydrogenase. The phosphate-dependent reduction of $NAD(P)^+$ with glyceraldehyde-3-phosphate was assayed in 0.8-ml mixtures containing 50 mM Tricine-NaOH (pH 8.5), 10 mM potassium phosphate, 2 mM DTT, 2 mM $MgCl_2$, and 1 mM glyceraldehyde-3-phosphate, as well as 10 mM methyl viologen, 1 mM NAD^+, or 1 mM $NADP^+$. The gas phase was 100% N_2. The reduction of $NAD(P)^+$ was monitored. The ATP-dependent reduction of 3-phosphoglycerate with NAD(P)H was determined in 0.8-ml assay mixtures containing morpholinepropanesulfonic acid (MOPS)-KOH (pH 7.0), 2 mM DTT, 2 mM $MgCl_2$, 1 mM ATP, 1 mM 3-phosphoglycerate, 10 U 3-phosphoglycerate kinase, and 0.2 mM NADH or 0.2 mM NADPH. The gas phase was 100% N_2. The oxidation of NAD(P)H was monitored.

Pyruvate:ferredoxin oxidoreductase. The 0.4-ml assay mixtures contained 100 mM potassium phosphate (pH 7.0), 2 mM DTT, 2 mM $MgCl_2$, 10 mM pyruvate, 0.1 mM coenzyme A, 1 mM thiamine pyrophosphate, 4 U phosphotransacetylase, and about 30 μM ferredoxin. The gas phase was 100% N_2. The reduction of ferredoxin was monitored.

Acetaldehyde dehydrogenase (CoA acetylating). The 0.8-ml assay mixture contained 100 mM MOPS-KOH (pH 7.0), 2 mM DTT, 2 mM $MgCl_2$, 1 mM acetyl phosphate, 1 mM coenzyme A, 10 U phosphotransacetylase, and 0.2 mM NADH or 0.2 mM NAPH. The gas phase was 100% N_2. The oxidation of NAD(P)H was monitored.

Ethanol dehydrogenase. The 0.8-ml assay mixtures contained 100 mM potassium phosphate (pH 7.0), 2 mM DTT, 2 mM $MgCl_2$, 1.25 mM acetaldehyde, and 0.2 mM NADH or 0.2 mM NADPH. The gas phase was 100% N_2. The oxidation of NAD(P)H was monitored.

Acetyl-CoA and ferredoxin-dependent H_2 formation from NADH. The 1-ml assay mixtures in 6.5-ml serum bottles contained 100 mM MOPS-KOH (pH 7.0), 2 mM DTT, 2 mM $MgCl_2$, 10 μM FAD, 10 μM FMN, 10 μM ferredoxin, an acetyl-CoA-regenerating system (20 mM acetyl phosphate, 0.5 mM coenzyme A, and 5 U phosphotransacetylase), and an NADH-regenerating system (2.5 mM NADH, 20 mM galactose, and 1 U galactose dehydrogenase). H_2 formation was monitored.

Reduced ferredoxin:NAD(P) oxidoreductase. The assay mixtures contained 100 mM potassium phosphate (pH 7.0), 2 mM DTT, 2 mM $MgCl_2$, 10 μM ferredoxin, 0.1 U ferredoxin-dependent carbon monoxide dehydrogenase (15 μl cell extract of *M. thermoacetica*) (24), and 1 mM NAD^+ or $NADP^+$. The gas phase was 100% CO. The reduction of NAD(P) was monitored.

Acetaldehyde:ferredoxin oxidoreductase. The 0.8-ml assay mixtures contained 100 mM Tris-HCl (pH 7.5), 2 mM DTT, 2 mM $MgCl_2$, 1.25 mM acetaldehyde, and about 30 μM ferredoxin or 10 mM methyl viologen. The gas phase was 100% N_2. Ferredoxin reduction or methyl viologen reduction was monitored.

Formate dehydrogenase. The reduction of methyl viologen with formate was assayed in 0.8-ml mixtures containing 100 mM potassium phosphate (pH 7.0), 2 mM DTT, 2 mM $MgCl_2$, 20 mM sodium formate, and 10 mM methyl viologen. The gas phase was 100% N_2. The formation of H_2 from formate was determined in 1-ml assay mixtures containing 100 mM potassium phosphate (pH 7.0), 2 mM DTT, 2 mM $MgCl_2$, and 20 mM sodium formate.

Ferredoxin-dependent transhydrogenase. The assay mixtures contained 100 mM MOPS-KOH (pH 7.0), 2 mM DTT, 2 mM $MgCl_2$, 10 μM FAD, 0.5 mM $NADP^+$, 40 mM glucose-6-phosphate, 2 U glucose-6-phosphate dehydrogenase (NADPH-regenerating system), 10 mM NAD^+, and about 30 μM ferredoxin. The gas phase was 100% N_2. The reduction of ferredoxin was monitored.

Ferredoxin-dependent hydrogenase. The reduction of ferredoxin with H_2 was assayed in 0.4-ml mixtures containing 100 mM Tris-HCl (pH 7.5), 2 mM DTT, 2 mM $MgCl_2$, and about 30 μM ferredoxin. The gas phase was 100% H_2. The formation of H_2 from reduced ferredoxin was determined using 1-ml assay mixtures containing 100 mM potassium phosphate (pH 7.0), 2 mM DTT, 2 mM $MgCl_2$, and a reduced ferredoxin-regenerating system (10 μM ferredoxin, 0.1 U pyruvate:ferredoxin oxidoreductase, 10 mM pyruvate, 1 mM thiamine pyrophosphate, 0.1 mM coenzyme A, and 2 U phosphotransacetylase). The gas phase was 100% N_2.

Ferredoxin- and NAD-dependent hydrogenase. The reduction of $NAD(P)^+$ and ferredoxin with H_2 was assayed in 0.4-ml mixtures containing 100 mM Tris-HCl (pH 7.5), 2 mM DTT, 2 mM $MgCl_2$, about 30 μM ferredoxin, and 1 mM NAD^+ or 1 mM $NADP^+$. The gas phase was 100% H_2. The formation of H_2 from reduced ferredoxin and NAD(P)H was determined using 1-ml assay mixtures containing 100 mM potassium phosphate (pH 7.0), 2 mM DTT, 2 mM $MgCl_2$, and 1 mM NADH or 1 mM NADPH and the reduced ferredoxin-regenerating system described above. The gas phase was 100% N_2.

Methyl viologen-reducing hydrogenase activity. Methyl viologen reduction with H_2 was assayed in 0.8-ml mixtures containing 100 mM Tris-HCl (pH 7.5), 2 mM DTT, 2 mM $MgCl_2$, and 10 mM methyl viologen. The gas phase was 100% H_2. The formation of H_2 from reduced methyl viologen was determined in assay mixtures containing 100 mM potassium phosphate (pH 7.0), 2 mM DTT, 2 mM $MgCl_2$, and a reduced methyl viologen-regenerating system (0.1 mM methyl viologen, 0.1 U pyruvate:ferredoxin oxidoreductase, 10 mM pyruvate, 1 mM thiamine pyrophosphate, 0.1 mM coenzyme A, and 4 U phosphotransacetylase). The gas phase was 100% N_2.

Enzyme purification. All purifications were carried out under strictly anoxic conditions at room temperature in a type B vinyl anaerobic chamber (Coy, Grass Lake, MI), which was filled with 95% N_2 and 5% H_2 and contained a palladium catalyst for O_2 reduction with H_2. The materials for protein purification all were obtained from GE Healthcare (Freiburg, Germany). The basal purification buffer used for column equilibration and elution was anoxic 50 mM Tris-HCl (pH 7.6) containing 1 mM sodium dithionite, 2 mM DTT, and 10 μM FMN.

Ferredoxin- and NAD-dependent hydrogenase. Cell extract of *R. albus* 7 (150,000 × *g* for the supernatant; 9.4 ml; 20 mg protein per ml) was supplemented with ammonium sulfate to a final concentration of 0.8 M and subsequently loaded onto a Phenyl-Sepharose high-performance column (1.6 by 14 cm) equilibrated with basal purification buffer containing 0.8 M ammonium sulfate. Protein was eluted with a combined stepwise and linear ammonium sulfate gradient (0.8 M, 90 ml; 0.8 to 0.68 M, 150 ml; 0.48 M, 90 ml; 0.48 to 0.32 M, 450 ml; 0.32 M, 30 ml; 0.32 to 0.16 M, 60 ml; and 0 M, 90 ml) at a flow rate of 2 ml min^{-1}. The ferredoxin-dependent hydrogenase activity eluted in a peak at 0.6 M, and the NAD- and ferredoxin-dependent hydrogenase activity eluted in a peak at 0.46 M ammonium sulfate. The latter fractions were pooled, concentrated, and desalted with an Amicon cell with a 30-kDa-cutoff membrane. The concentrate then was applied onto a DEAE-Sepharose high-performance column (1.6 by 19 cm) equilibrated with basal buffer containing 5% glycerol. Protein was eluted with a combined stepwise and linear NaCl gradient (0 M, 80 ml; 0.1 M, 80 ml; 0.1 to 0.2 M, 120 ml; 0.2 to 0.3 M, 400 ml; 0.3 to 0.4 M, 120 ml; and 1 M, 120 ml) at a flow rate of 3 ml min^{-1}. The hydrogenase activity was recovered in a peak eluting around 0.22 M NaCl. The fraction was concentrated and desalted with a 30-kDa-cutoff Amicon membrane.

The concentrate then was applied onto a Q Sepharose high-performance column (1.6 by 15 cm) equilibrated with basal buffer containing 5% glycerol. Protein was eluted with a combined stepwise and linear NaCl gradient (0 M, 60 ml; 0.1 M, 60 ml; 0.1 to 0.2 M, 90 ml; 0.2 to 0.25 M, 300 ml; 0.25 to 0.3 M, 150 ml; and 1 M, 90 ml) at a flow rate of 2 ml min^{-1}. The hydrogenase activity appeared at around 0.23 M NaCl. The fractions were combined, concentrated, and desalted with a 30-kDa-cutoff Amicon membrane. During purification, the rate of methyl viologen reduction with H_2 and the protein concentrations were monitored.

Pyruvate:ferredoxin oxidoreductase. Cell extract of *R. albus* 7 (150,000 × *g* for the supernatant; 10 ml; about 20 mg protein per ml) was supplemented with ammonium sulfate to a final concentration of 0.8 M and subsequently loaded onto a Phenyl-Sepharose high-performance column (1.6 by 14 cm) equilibrated with basal buffer containing 0.8 M ammonium sulfate and 0.1 mM thiamine pyrophosphate. The column subsequently was washed with 150 ml of the equilibration buffer, and then protein was eluted with a 0.8 to 0.68 M ammonium sulfate linear gradient at a flow rate of 2 ml min^{-1}. Pyruvate:ferredoxin oxidoreductase activity was recovered in fractions eluting near 0.75 M ammonium sulfate. The fractions were devoid of hydrogenase activity as tested via methyl viologen reduction with H_2.

Identification of proteins via their amino acid sequence. Proteins were analyzed either directly or after separation on SDS-12% polyacrylamide gels and staining with Coomassie brilliant blue G250. The proteins were digested with sequencing-grade modified trypsin (Promega, Mannheim, Germany), and the resulting peptide mixture was injected into a PepMap100 C_{18} reverse-phase nanocolumn (Dionex, Idstein, Germany) and separated on an UltiMate 3000 liquid chromatography system (Dionex). Peptides were analyzed by matrix-assisted laser desorption ionization–time of flight tandem mass spectrometry (MALDI-TOF MS/MS). The MS and MS/MS data were searched against an in-house protein database using Mascot embedded into GPS explorer software (MDS Sciex) (26).

Analysis of transcription by reverse transcription-PCR (RT-PCR). Total RNA was extracted from *R. albus* 7 cells grown exponentially on glucose with TRIzol reagent (Invitrogen, Darmstadt, Germany) according to the manufacturer's protocol. The resulting RNA was treated with RNase-free DNase I (Fermentas, St. Leon-Rot, Germany) at 37°C for 2 h after its integrity was checked by agarose electrophoresis (43). The DNase I-digested RNA was used next to synthesize first-strand cDNA using Transcriptor reverse transcriptase (Roche, Mannheim, Germany) and random hexamer primers according to the manufacturer's protocol. The resulting cDNA was used as the template to amplify the intragenic regions of *hydB*, *hydA2*, and *hydS* genes for transcriptional analysis, and the intergenic regions of the *Rumal_3398-3408* gene cluster were used to analyze cotranscription. Genomic DNA and total RNA were used as positive and negative controls, respectively (25). The specific primers used for amplification are listed in Table S1 in the supplemental material.

Nucleotide sequence accession numbers. The *R. albus* 7 genome GenBank accession number is CP002403.1, and the *R. albus* 7 plasmids pRumal01, pRumal02, pRumal03, and pRumal04 GenBank accession numbers are CP002404.1, CP002405.1, CP002406.1, and CP002407.1, respectively.

RESULTS

Before analyzing and characterizing the three hydrogenases in *R. albus* 7, we report on the genes and specific activities of all oxidoreductases that might be involved in the fermentation of glucose in order to be able to understand what function the individual hydrogenases could have.

Genes present for glucose fermentation. *R. albus* 7 ferments glucose to acetic acid, ethanol, CO_2, H_2, and small amounts of formate (44), most probably involving the Embden-Meyerhoff pathway. In the genome (27), all of the genes required for this pathway and for the conversion of pyruvate to the various end products are present: a glucose-proton symporter, hexokinase, glucose-6-phosphate isomerase, phosphofructokinase, aldolase, triosephosphate isomerase, glyceraldehyde-3-phosphate isomerase, phosphoglycerate mutase, enolase, pyruvate kinase, pyruvate:ferredoxin oxidoreductases, pyruvate-formate lyase, phosphotransacetylase, acetokinase, two bifunctional acetaldehyde/ethanol dehydrogenases, and three [FeFe]-hydrogenases (HydABC, HydA2, and HydS). Genes for a glucose phosphoenolpyruvate (PEP) transferase transport system, for an ABC glucose transporter, and for a glucose diffusion facilitator were not found. Genes for a formate dehydrogenase also appear to be absent (see below).

Specific activities of oxidoreductases potentially involved in glucose fermentation. *R. albus* 7 was grown at 37°C in batch culture on glucose in the exponential phase with a doubling time of about 2 h and a cell yield of 33 g (dry mass) per mol glucose. Based on these findings and on a cellular protein content of about 50%, the cells consumed glucose in the exponential growth phase at a specific rate of about 0.3 μmol per min and mg protein. Acetate was formed at 1.3 times and H_2 at 2.6 times this specific rate. Therefore, the oxidoreductases involved in glucose fermentation should have specific activities in cell extracts consistent with these specific rates. This was found to be the case for NAD-specific glyceraldehyde-3-phosphate dehydrogenase, pyruvate:ferredoxin oxidoreductase, NAD-specific acetaldehyde dehydrogenase, NAD-specific ethanol dehydrogenase, ferredoxin-dependent hydrogenase, and ferredoxin- and NAD-dependent hydrogenase (Table 1). The specific activities of all other oxidoreductases tested were at least an order of magnitude lower.

Glyceraldehyde-3-phosphate dehydrogenase. Cell extracts catalyzed the phosphate-dependent reduction of NAD^+ with glyceraldehyde-3-phosphate at a specific activity of 1.7 U/mg protein (Table 1). With $NADP^+$, the specific activity was less than 0.1 U/mg. In the absence of phosphate, neither NAD^+ nor $NADP^+$ was reduced (not shown). Ferredoxin was not used as an electron acceptor for glyceraldehyde-3-phosphate dehydrogenation in either the presence or absence of phosphate. Consistent with this, genes for a nonphosphorylating NAD(P)-dependent glyceraldehyde-3-phosphate dehydrogenase (45, 46) and a glyceraldehyde-3-phosphate:ferredoxin oxidoreductase (47, 48) do not appear to be present. In the genome of *R. albus* 7, only one gene for an NAD^+- and phosphate-dependent glyceraldehyde-3-phosphate dehydrogenase is found. The deduced amino acid sequence has a high level of sequence identity to that of its counterpart in other Gram-positive bacteria.

Pyruvate:ferredoxin oxidoreductase. Under standard assay conditions the cell extracts catalyzed the CoA-dependent reduction of ferredoxin with pyruvate at a specific activity of 1.0 U per mg (Table 1). NAD^+ and $NADP^+$ were not reduced by pyruvate. Consistent with this, in the genome of *R. albus* 7, only a gene for a pyruvate:ferredoxin oxidoreductase is found rather than the genes for a pyruvate dehydrogenase complex. The deduced amino acid sequence has a high level of sequence identity to the monomeric pyruvate:ferredoxin oxidoreductases present in *A. woodii*, *M. thermoacetica*, and *C. pasteurianum*, which have three [4Fe4S] clusters and a thiamine pyrophosphate binding site.

Bifunctional acetaldehyde/ethanol dehydrogenase. Cell extracts catalyzed the reduction of acetyl-CoA and of acetaldehyde with NADH at specific rates of 1.1 U/mg and 1.9 U/mg, respectively (Table 1). The specific rates with NADPH were at least an

TABLE 1 Cofactor specificities and specific activities of fermentation-related oxidoreductases in cell extract of *R. albus* 7[e]

Enzyme activity and substrate(s) tested	Product(s) monitored	Sp act[f] (U/mg)
Glyceraldehyde-3-phosphate dehydrogenase		
GAP + P_i + NAD^+	NADH	**1.7**
GAP + P_i + $NADP^+$	NADPH	<0.1
1,3-BPG[a] + NADH	NADH	6.0
1,3-BPG[a] + NADPH	NADPH	0.1
GAP + MV_{ox}	MV_{red}	<0.1
Pyruvate:ferredoxin oxidoreductase: Pyr + Fd_{ox} + CoA	Fd_{ox}	**1.0**
Acetaldehyde DH (CoA acetylating)		
Acetyl-CoA[b] + NADH	NADH	**1.1**
Acetyl-CoA[b] + NADPH	NADPH	0.02
Ethanol dehydrogenase		
AcH + NADH	NADH	**1.9**
AcH + NADPH	NADPH	0.02
Acetyl-CoA and ferredoxin-dependent H_2 formation from NADH		
NADH + Fd_{ox} + acetyl-CoA[b]	H_2	0.03
NADH + Fd_{ox}	H_2	<0.01
Reduced ferredoxin:NAD(P) oxidoreductase: Fd_{red}[c] + $NAD(P)^+$	NAD(P)H	<0.01
Acetaldehyde oxidoreductase		
AcH + MV_{ox}	MV_{red}	<0.01
AcH + Fd_{ox}	Fd_{ox}	<0.01
Formate dehydrogenase		
Formate + MV_{ox}	MV_{red}	<0.01
Formate	H_2	<0.01
Ferredoxin-dependent transhydrogenase: NADPH + NAD^+ + Fd_{ox}	Fd_{ox}	0.05
Ferredoxin-dependent hydrogenase		
Fd_{red}[d]	H_2	**0.3**
H_2 + Fd_{ox}	Fd_{ox}	0.1
H_2 + $NAD(P)^+$	NAD(P)H	<0.01
Ferredoxin- and NAD-dependent hydrogenase		
NADH + Fd_{red}[d]	H_2	**0.6**
NADH	H_2	<0.01
NADPH + Fd_{red}[d]	H_2	0.3
H_2 + NAD^+ + Fd_{ox}	NADH	1.6
H_2 + $NADP^+$ + Fd_{ox}	NADPH	<0.1

[a] 1,3-BPG-regenerating system: 3-phosphoglycerate, ATP, and 3-phosphoglycerate kinase.
[b] Acetyl-CoA-regenerating system: acetyl phosphate, coenzyme A, and phosphotransacetylase.
[c] Fd_{red}-regenerating system I: ferredoxin, ferredoxin-dependent CO dehydrogenase, and CO.
[d] Fd_{red}-regenerating system II: ferredoxin, pyruvate:Fd oxidoreductase, pyruvate, coenzyme A, inorganic phosphate, and phosphotransacetylase.
[e] *R. albus* 7 was grown in batch culture on glucose. For assay conditions, see Materials and Methods. Fd, ferredoxin; MV, methyl viologen; GAP, glyceraldehyde-3-phosphate; P_i, inorganic phosphate; 1,3-BPG, 1,3-bisphosphoglycerate; Pyr, pyruvate; DH, dehydrogenase; AcH, acetaldehyde.
[f] Boldface indicates relevant specific activities.

order of magnitude lower. Ferredoxin or methyl viologen were not reduced by acetaldehyde in either the absence or presence of CoA; this indicated the absence of an aldehyde:ferredoxin oxidoreductase, which is a molybdopterin-dependent enzyme (49). Consistent with this, the genome of *R. albus* lacks the gene for an aldehyde:ferredoxin oxidoreductase and also several genes essential for molybdopterin biosynthesis. However, the genome harbors two genes for two bifunctional acetaldehyde/ethanol dehydrogenases (50), one located on the chromosome and the other on the plasmid pRumal01. Both genes were expressed under the culture conditions revealed from the amino acid sequence of the partially purified bifunctional enzymes.

Besides the two genes for the two bifunctional acetaldehyde/ethanol dehydrogenases, the genome harbors genes for a monofunctional CoA-dependent acetaldehyde dehydrogenase and for two monofunctional alcohol dehydrogenases. It remains unclear whether these dehydrogenases are connected to the reduction of acetyl-CoA with NADH to ethanol.

Acetyl-CoA-dependent H_2 formation from NADH. It has been reported (16) that cell extracts of *R. albus* catalyze the ferredoxin- and acetyl-CoA-dependent formation of H_2 from NADH at very low specific rates. We confirmed this observation (Table 1) without having an explanation for which gene products could be involved. The genome of *R. albus* lacks genes for enzymes catalyzing the reduction of acetyl-CoA to butyryl-CoA, which in cell extracts of butyric-acid-forming clostridia are responsible for the reported acetyl-CoA- and ferredoxin-dependent H_2 formation from NADH. In butyric-acid-forming clostridia, all of which contain a ferredoxin-dependent [FeFe]-hydrogenase, the exergonic reduction of crotonyl-CoA with NADH is coupled with the endergonic reduction of ferredoxin with NADH (51, 52). The coupled reaction is catalyzed by an enzyme complex of butyryl-CoA dehydrogenase with the electron transfer flavoproteins EtfA and EtfB.

In *A. woodii*, the exergonic reduction of pyruvate with NADH to lactate is coupled with the endergonic reduction of ferredoxin with NADH (53). The reaction is catalyzed by a lactate dehydrogenase in complex with the electron transfer flavoproteins EtfA and EtfB. The reduction of acetaldehyde with NADH to ethanol is thermodynamically equivalent to the reduction of pyruvate with NADH to lactate. Therefore, in principle, the acetyl-CoA- and ferredoxin-dependent formation of H_2 from NADH in cell extracts of *R. albus* (Table 1) could be due to the presence of a ferredoxin- and NAD-dependent alcohol dehydrogenase. However, in the genome of *R. albus* 7, genes for the electron transfer flavoproteins EtfA and EtfB, thought to be involved in the coupling mechanism, are not found (52–54).

Reduced ferredoxin:NAD oxidoreductase. In many anaerobes, the membrane-associated complex RnfA-G catalyzes the reversible reduction of NAD^+ with reduced ferredoxin and couples the exergonic reaction with the build-up of a proton or sodium ion motive force (22, 55). Such an activity was not found in *R. albus* (Table 1). In the genome of *R. albus* 7, genes for RnfC (NADH dehydrogenase) and RnfD (FMN-containing membrane protein) are found in a transcriptional unit coding for a membrane-associated enzyme complex. However, the subunits of this complex, with the exception of RnfC and RnfD, show no sequence similarity to the subunits in the classical RnfA-G complex.

Formate dehydrogenase. Reports have been published (44) that formate in *R. albus* is formed from CO_2; this indicates the presence of reversible formate dehydrogenases which are molyb-

dopterin-containing enzymes (56). The cell extracts did not catalyze the reduction of ferredoxin or methyl viologen with formate. Consistent with this, the genome lacks a gene for a reversible formate dehydrogenase and several genes essential for the synthesis of molybdopterin. However, the genome carries all genes required for expression of a functional pyruvate-formate lyase. Therefore, the lyase most probably is responsible for the reported formate formation (44).

Carbon monoxide dehydrogenase. Many Gram-positive anaerobic bacteria have the potential to reduce 2 CO_2 to acetic acid via the Wood-Ljungdahl pathway (57). One of the key enzymes is the ferredoxin-dependent carbon monoxide dehydrogenase (58). A similar activity was not found in the cell extracts (Table 1), although one of the three plasmids, namely, pRumal02, harbors a gene encoding a carbon monoxide dehydrogenase. However, the genome lacks genes for the key enzyme of this pathway, namely, acetyl-CoA synthase/decarbonylase.

Ferredoxin-dependent transhydrogenase. The genome of *R. albus* 7 harbors *nfnAB* genes for the synthesis of an electron-bifurcating transhydrogenase complex that couples the endergonic reduction of $NADP^+$ with NADH to the exergonic reduction of $NADP^+$ with reduced ferredoxin (24, 40). Only very low specific activities (0.05 U/mg) of this transhydrogenase could be detected in the cell extracts of *R. albus*. Therefore, we propose an anabolic rather than a catabolic function for this enzyme. Transhydrogenase activity in cell extracts of *R. albus* has been observed before (18).

Hydrogenases. Cell extracts catalyzed the formation of H_2 from reduced ferredoxin at a specific rate of 0.3 U/mg, which indicated the presence of a ferredoxin-dependent hydrogenase (Table 1). The specific rate increased to 0.6 U/mg in the presence of NADH (Table 1), which indicated the additional presence of a ferredoxin- and NAD-dependent hydrogenase at a specific activity of 0.3 U/mg. NADPH could not substitute for NADH.

Evidence for the presence of three [FeFe]-hydrogenases: HydA2, HydABC, and HydS. Two hydrogenase activities were separated by chromatography on Phenyl-Sepharose (see Materials and Methods). The activity that eluted first (0.6 M ammonium sulfate) coeluted with the *hydA2* gene product, and the activity that eluted second (0.46 M ammonium sulfate) coeluted with the *hydABC* gene products, as identified via mass spectrometry analysis of the proteins in the fractions.

The ferredoxin-dependent [FeFe]-hydrogenase HydA2 very rapidly lost activity upon dilution, even under strictly anoxic conditions, which in our hands made the purification of this enzyme impossible. After separation on Phenyl-Sepharose, only a small percentage of the activity determined in cell extracts remained. In contrast, the activity of the electron-bifurcating ferredoxin- and NAD-dependent [FeFe]-hydrogenase HydABC was relatively stable and could be purified easily (see below).

The lability of HydA2 relative to that of HydABC may have something to do with the second coordination sphere of the H-cluster (28, 29), which in HydA conforms to that in other [FeFe]-hydrogenases but which in HydA2 differs at six amino acid positions (Fig. 1). Mutational analyses revealed that several residues around the H-cluster are structurally relevant for the function and stability of the active site, especially those that show electrostatic or H-bond interactions with the CO and CN ligands, as well as the bridging ligand (28).

Before we knew that HydA2 rapidly lost its activity upon dilution, we sometimes recovered no ferredoxin-dependent hydrogenase activity after chromatography of the cell extract on Phenyl-Sepharose (described above). Therefore, we ascertained via RT-PCR analysis that both the *hydABC* genes on the chromosome and the *hydA2* gene on the plasmid pRumal01 were expressed during growth of *R. albus* on glucose, and this was found to be the case (Fig. 2).

Segment 1

Consensus	F L I	T	S	-	C	C	P	G A S	W	V
HydA	F	T	S	-	C	C	P	G	W	V
HydA2	L	T	S	S	C	C	P	A	F	V
HydS	I	S	S	-	C	C	H	S	-	V

Segment 2

Consensus	I V	T M	P	C	x	A S	K	K	x	E
HydA	V	I	P	C	T	A	K	K	F	E
HydA2	I	G	P	C	T	A	K	K	A	E
HydS	I	G	P	C	V	S	K	K	D	E

Segment 3

Consensus	I V	E	x	M	-	A	C	H N P	G	G	C	I	x	G	A G	G	T S Q	P
HydA	V	E	I	M	-	A	C	P	G	G	C	I	N	G	G	G	Q	P
HydA2	I	E	G	M	-	A	C	I	G	G	C	I	G	G	A	G	C	L
HydS	I	E	-	M	S	A	C	N	G	S	C	I	-	G	G	-	-	P

FIG 1 Three segments encompassing the four cysteine ligands (in red) involved in H-cluster iron binding in the three [FeFe]-hydrogenases of *R. albus*. The consensus sequence in the three segments is based on the review by Lubitz et al. (28). Underlined letters indicate fully conserved residues; an "x" indicates that more than four different residues are found at that position. HydA is subunit A of the electron-bifurcating ferredoxin- and NAD-dependent [FeFe]-hydrogenase HydABC; HydA2 is the ferredoxin-dependent [FeFe]-hydrogenase; HydS is the putative H_2-sensing [FeFe]-hydrogenase. HydA2 has 27% (83% coverage) and HydS 26% (52% coverage) sequence identity to HydA, and HydA has 42% sequence identity to the [FeFe]-hydrogenase I from *C. pasteurianum*.

During purification of HydABC and separation from HydA2, we carefully looked for a third hydrogenase activity peak due to HydS by measuring the reduction of methyl viologen with H_2, but without success. The HydABC- and HydA2-containing fractions also did not appear to contain HydS, as revealed by mass spectrometry of the proteins in the fractions. We could show, however, via RT-PCR analysis that the *hydS* gene on plasmid pRumal01 was expressed under the experimental conditions (Fig. 2). Since the second coordination sphere of the H-cluster in HydS differs at 10 amino acid positions from that of bona fide [FeFe]-hydrogenases (Fig. 1), it is difficult to predict whether HydS has very low or no hydrogenase activity or whether HydS is just more labile than metabolic [FeFe]-hydrogenases.

The genome of *R. albus* does not harbor genes for [NiFe]-hydrogenase. Of the eight genes required for the maturation of [NiFe]-hydrogenases, only four (*hypC*, *hypD*, *hypE*, and *hypF*) were found (28, 59).

Purification and properties of the electron-bifurcating [FeFe]-hydrogenase HydABC. As mentioned above, the ferredoxin- and NAD-dependent hydrogenase activity in cell extracts was relatively stable. To determine the stoichiometry of coupling, we purified the enzyme 37-fold via chromatography on Phenyl-Sepharose, DEAE-Sepharose, and Q Sepharose at a yield of 15% and a specific activity of 60 U per mg protein (Table 2).

SDS-PAGE revealed that the preparation is composed mainly of three proteins, which were identified via mass spectrometry as HydA, HydB, and HydC (Fig. 3). Mass spectrometric analysis of a fourth protein band migrating with an apparent molecular mass

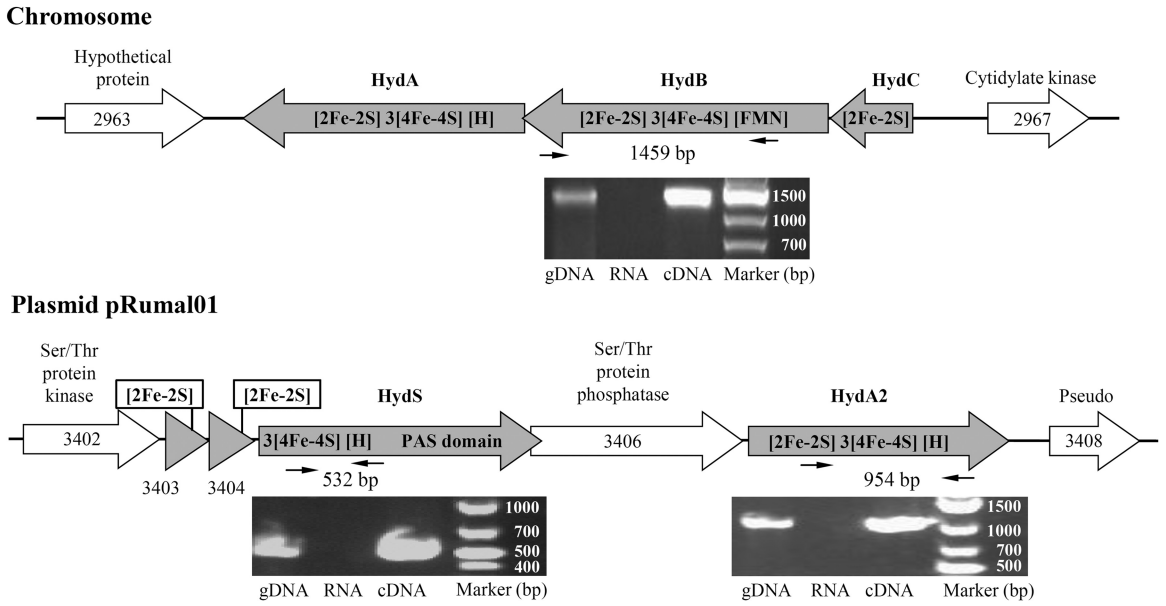

FIG 2 *R. albus* chromosomal region encoding the electron-bifurcating ferredoxin- and NAD-dependent [FeFe]-hydrogenase HydABC and the region on plasmid pRuma101 encoding the ferredoxin-dependent [FeFe]-hydrogenase HydA2 and putative H_2-sensing [FeFe]-hydrogenase HydS. The cofactor content was predicted from the amino acid sequence of the proteins. RT-PCR analysis revealed that the genes for HydA, HydA2, and HydS are expressed during growth of *R. albus* 7 in batch culture on glucose. gDNA, genomic DNA; RNA, total RNA. The numbers in the scheme correspond to numbers in *Rumal_3402* to *Rumal_3408* locus tags.

of about 100 kDa identified it as a mixture of the bifunctional acetaldehyde/ethanol dehydrogenases encoded by the chromosome and of the bifunctional enzyme encoded by the plasmid pRumal01.

The purified enzyme complex catalyzed the reduction of NAD^+ and of the two-electron-accepting ferredoxin from *C. pasteurianum* with H_2 in an almost 1:1 stoichiometry (Fig. 4). $NADP^+$ was not reduced. In an assay system in which reduced ferredoxin was continuously regenerated by reduction with pyruvate in the presence of purified pyruvate:ferredoxin oxidoreductase and CoA, the formation of H_2 was strictly dependent on NADH. NADPH could not substitute for NADH (not shown).

Cotranscription of the genes for HydA2 and HydS. Evidence for cotranscription comes from bioinformatics and from experimental RT-PCR analysis (Fig. 5). Bioinformatic analysis of the genes neighboring *hydA2* and *hydS* indicates that both genes are part of a transcriptional unit, starting with gene *rstR*, which encodes the redox-sensing transcriptional repressor Rex and ends with a pseudogene. The putative transcription unit also carries genes for a serine/threonine protein kinase and a serine/threonine protein phosphatase (60, 61), a bifunctional acetaldehyde/ethanol dehydrogenase, and two iron-sulfur proteins, each containing a [2Fe2S]-cluster. Using the BPROM online program (62) and ARNold online program (63–66), we identified, upstream of the cluster, a putative terminator sequence followed by a promoter sequence, and, downstream of the cluster, two putative terminator sequences. Within the cluster, no such sequences are apparent.

TABLE 2 Purification of the electron-bifurcating ferredoxin- and NAD-dependent [FeFe]-hydrogenase from *R. albus* 7[a]

Purification step	Protein (mg)	NAD^+-dependent ferredoxin reduction with H_2[b]			
		U	U/mg	Yield (%)	Purification factor
Cell extract	190	300	1.6	100	1
Phenyl-Sepharose	5.5	156	28	52	17.8
DEAE-Sepharose	1.9	48	25	16	15.8
Q Sepharose	0.7	44	60	15	37.2

[a] *R. albus* 7 grown in batch culture on glucose.
[b] One unit = 1 μmol per min.

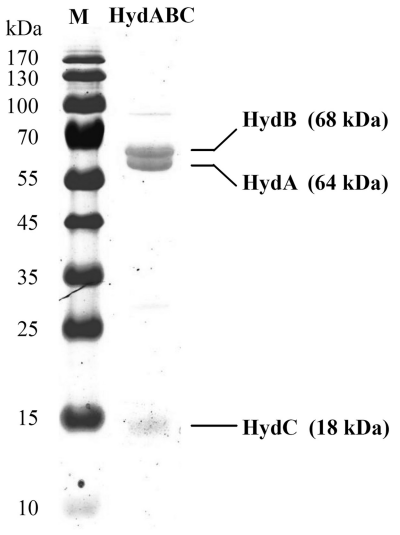

FIG 3 SDS-PAGE of purified electron-bifurcating ferredoxin- and NAD-dependent [FeFe]-hydrogenase (HydABC) from *R. albus*. The protein-coding genes were identified via mass spectrometry. The minor protein band at 100 kDa is due to a contaminating bifunctional acetaldehyde/ethanol dehydrogenase.

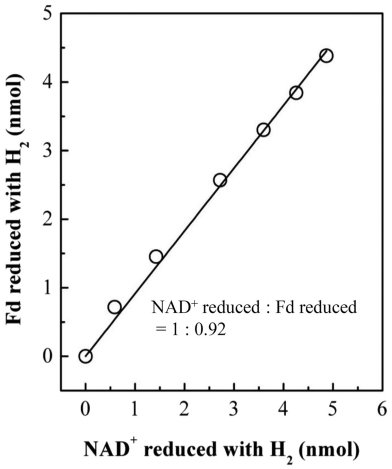

FIG 4 Stoichiometry of ferredoxin and NAD reduction by H_2 catalyzed by purified electron-bifurcating ferredoxin- and NAD-dependent [FeFe]-hydrogenase from *R. albus* 7. In the experiment, ferredoxin from *C. pasteurianum* was used, which harbors two [4Fe4S] clusters and accepts two electrons at almost the same redox potential of −400 mV (87). The ferredoxin of *C. pasteurianum* is very similar to that of *R. albus* (19).

RT-PCR analysis revealed that these genes indeed form a transcriptional unit (Fig. 5). Directly upstream of the transcriptional unit lies the gene *lysR*, which is predicted to code for a transcriptional regulator of the LysR family (67); directly downstream of the transcription unit lies a gene encoding an AAA-ATPase (68).

DISCUSSION

The results presented were obtained with *R. albus* strain 7. The other two *R. albus* strains sequenced are strains 8 and SY3, both of which harbor the genes *hydABC*, encoding the electron-bifurcating ferredoxin- and NAD-dependent [FeFe]-hydrogenase, the gene *hydA2*, encoding ferredoxin-dependent [FeFe]-hydrogenase, and the gene *hydS*, encoding the putative H_2-sensing [FeFe]-hydrogenase. In the three *R. albus* strains, the arrangements of the genes in the neighborhood of *hydA2* and *hydS* are identical. The sequences of the electron-bifurcating ferredoxin- and NAD-dependent [FeFe]-hydrogenases of the three strains are over 90% identical. However, the enzyme from strain 8 is predicted to be composed of four rather than three subunits, with the *hydB* gene being split in two. The amino acid sequences of glyceraldehyde-3-phosphate dehydrogenase, pyruvate:ferredoxin oxidoreductase, and bifunctional acetaldehyde/ethanol dehydrogenase in strains 7, 8, and SY3 are over 90% identical. Based on all of these findings, we concluded that all strains of *R. albus* ferment cellulose, cellobiose, or glucose and regulate product formation in a similar manner. The fermentation scheme for glucose, which is fermented only by *R. albus* 7, is outlined in Fig. 6.

When *R. albus* 7 ferments glucose, ethanol, acetic acid, CO_2, and H_2 are formed according to the following reaction: glucose + $(2 - a)$ $H_2O \rightarrow a$ ethanol + 2 CO_2 + $(2 - a)$ acetate$^-$ + $(2 - a)$ H^+ + $(4 - 2a)$ H_2, where a is a number between 0 and 1 (Fig. 6). At very high H_2 partial pressure, 1 ethanol, 1 acetic acid, 2 CO_2, and 2 H_2 are formed as products, $a = 1$, and all of the H_2 is generated via the ferredoxin-dependent hydrogenase HydA2. At very low H_2 partial pressures, 2 acetic acid, 2 CO_2, and 4 H_2 are formed as products, $a = 0$, and all of the H_2 is generated via the electron-bifurcating ferredoxin- and NAD-dependent [FeFe]-hydrogenase HydABC. In batch fermentations, 0.7 ethanol, 1.3 acetic acid, 2 CO_2, and 2.6 H_2 are formed, $a = 0.7$, and 1.2 mol of the H_2 formed was generated via the electron-bifurcating [FeFe]-hydrogenase HydABC; 1.4 mol was generated via the ferredoxin-dependent [FeFe]-hydrogenase HydA2 (Fig. 6).

Fermentation of glucose to 2 ethanol and 2 CO_2 ($a = 2$) in *R. albus* is not possible, since the organism appears to lack a reduced ferredoxin:NAD^+ oxidoreductase that would allow the transfer of electrons from reduced ferredoxin to NAD^+ (Table 1). This has to be kept in mind when considering the engineering of *R. albus* for second-generation bioethanol production so that it can ferment cellulose to 2 ethanol and 2 CO_2 per hexose unit without the generation of acetic acid and H_2 (69). The ability of *R. albus* to hydrolyze and ferment the major plant cell wall polysaccharides, cel-

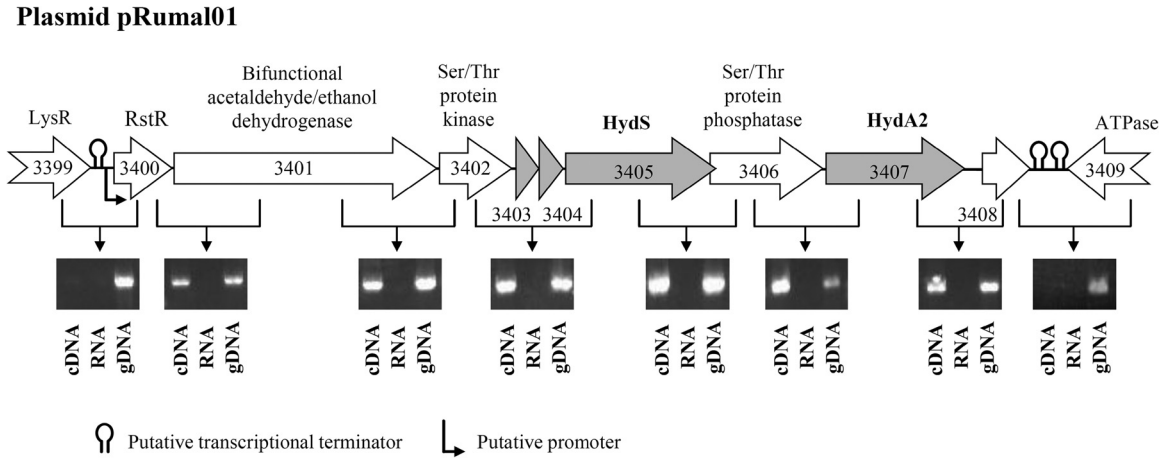

FIG 5 Cotranscriptional analysis of the *R. albus* 7 plasmid genes encoding the ferredoxin-dependent [FeFe]-hydrogenase HydA2 and the putative H_2-sensing [FeFe]-hydrogenase HydS, together with genes encoding the redox-sensing transcriptional repressor RstR, a bifunctional ethanol/acetaldehyde dehydrogenase, a serine/threonine protein kinase, a serine/threonine protein phosphatase, and a transposase pseudogene (Rumal_3408). Evidence for cotranscription comes from bioinformatic analysis (see the text) and from RT-PCR analyses of cells grown in batch culture on glucose. gDNA, genomic DNA; RNA, total RNA; LysR, transcriptional regulator; ATPase, putative AAA superfamily ATPase. The numbers in the arrows correspond to numbers in *Rumal_3399* to *Rumal_3409* locus tags.

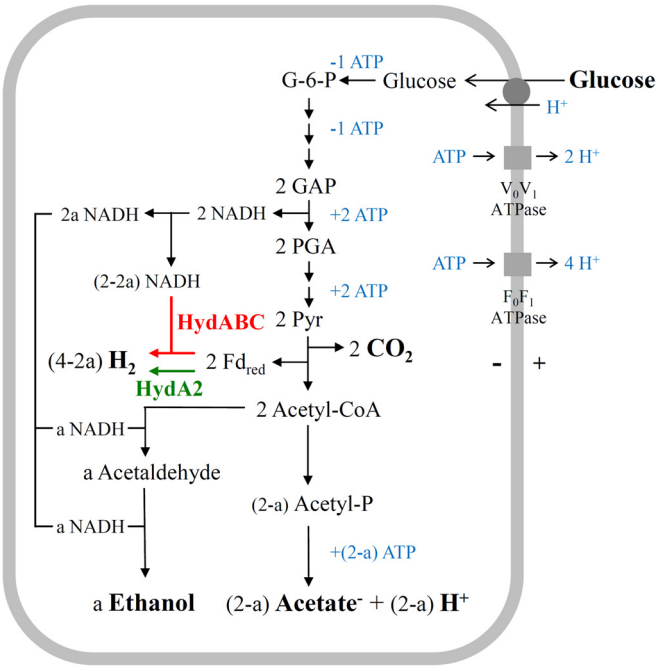

FIG 6 Scheme of the energy metabolism of *R. albus* 7 growing on glucose at low ($a = 0$) and at very high ($a = 1$) H_2 partial pressures. The relevant reaction is glucose + $(2 - a)$ $H_2O \rightarrow 2a$ ethanol + 2 CO_2 + $(2 - a)$ acetate$^-$ + $(2 - a)$ H^+ + $(4 - 2a)$ H_2. HydABC (highlighted in red) is the electron-bifurcating ferredoxin- and NAD-dependent [FeFe]-hydrogenase, and HydA2 (highlighted in green) is the ferredoxin-dependent [FeFe]-hydrogenase. G-6-P, glucose-6-phosphate; GAP, glyceraldehyde phosphate; PGA, phosphoglycerate; Pyr, pyruvate. The presence of the three membrane protein complexes is deduced from the genome sequence (27).

lulose and hemicellulose, is the reason for the renewed biotechnological interest in this organism (4, 69).

As described above, in batch cultures of *R. albus* grown on glucose, the electron-bifurcating ferredoxin- and NAD-dependent [FeFe]-hydrogenase HydABC and the ferredoxin-dependent [FeFe]-hydrogenase HydA2 are operative ($a = 0.7$) (Fig. 6). In contrast, during growth of *R. albus* in its natural gut environment, where the H_2 partial pressure is low, only the electron-bifurcating hydrogenase is required ($a = 0$) (Fig. 6). Under these conditions, the ferredoxin-dependent hydrogenase HydA2 and the bifunctional acetaldehyde/ethanol dehydrogenase do not need to be synthesized. Therefore, it probably is not random chance that the gene encoding HydA2 and the gene encoding the bifunctional acetaldehyde/ethanol dehydrogenase are located together in one transcriptional unit together with the *rstR* gene, encoding a redox-sensing transcriptional repressor, Rex.

Rex proteins have been implicated in the transcriptional regulation of genes that are important for fermentative growth and for growth under low oxygen tension, mainly in Gram-positive bacteria but also in some Gram-negative bacteria. Rex senses the redox poise of the cell through changes in the NADH/NAD^+ ratio (70–73). Rex has been shown to be involved in the response of the thermophilic Gram-positive anaerobe *Caldicellulosiruptor saccharolyticus* to different H_2 partial pressures (74). Therefore, it is conceivable that in *R. albus* the NADH/NAD^+ ratio somehow reflects the H_2 concentration in the environment, with the ratio being higher at high H_2 concentrations than at low H_2 concentrations. However, NADH and H_2 are not in thermodynamic equilibrium, since in the cells the redox potential, E′, of the NAD^+/NADH couple (near −280 mV) is predicted to be more positive than that of the $2H^+/H_2$ couple even when the H_2 partial pressure is only about 10 Pa (E′ near −310 mV). Therefore, the H_2 partial pressure must be sensed somehow and the signal transmitted such that the NADH/NAD^+ ratio is affected.

What could the H_2 sensor be? The *hydS* gene product is the most likely candidate for the following reasons. (i) HydS harbors an H-cluster to which H_2 can bind and transfer electrons; in addition, it harbors a PAS domain which could promote signal transfer (30). (ii) The *hydS* gene is in a transcriptional unit together with *hydA2*, encoding the ferredoxin-dependent [FeFe]-hydrogenase, and *rstR*, encoding the redox-sensing transcriptional repressor Rex. This transcriptional unit also carries genes for a serine/threonine protein kinase and a serine/threonine protein phosphatase, which could be involved in signal transfer (60, 61, 75). (iii) Directly upstream of the transcriptional unit lies a gene encoding a transcriptional regulator of the LysR family, which represents the most abundant type of transcriptional regulator in the prokaryotic kingdom (67). (iv) [FeFe]-hydrogenases with a PAS domain are found in many H_2-forming bacteria containing both a ferredoxin-dependent [FeFe]-hydrogenase and an electron-bifurcating ferredoxin- and NAD-dependent [FeFe]-hydrogenase. *Thermotoga maritima* (76), *Clostridium stercorarium* (77), *Clostridium thermocellum* (78), *Elusimicrobium minutum* (79), *Treponema azotonutricium* (33), and *Thermoanaerobacterium saccharolyticum* (35) are among these H_2-forming bacteria, which putatively respond to changing H_2 partial pressures in their environment by changing the pattern of fermentation products. In these organisms, the *hydS* gene also is associated with genes encoding transcriptional regulators (Rex or LysR), a serine/threonine protein kinase, and/or a serine/threonine protein phosphatase (Fig. 7). (v) The H-cluster in HydS from all of the bacteria mentioned above differs in the second coordination sphere from the H-cluster of metabolic [FeFe]-hydrogenases, such as HydA2 and HydABC (see Fig. S2 in the supplemental material), which indicates differences in reactivity and function from metabolic [FeFe]-hydrogenases. Genetic experiments, which have already been initiated with *T. saccharolyticum* (35), will be required to prove that HydS (HfsB in *T. saccharolyticum*) is a H_2-sensing, regulatory [FeFe]-hydrogenase and to find out how the signal is transferred and how it leads to the transcriptional response. It should be noted that *Caldicellulosiruptor saccharolyticus* (described above) can adapt to different H_2 partial pressures without having an *hydS* gene, which indicates that the mechanism of H_2 sensing differs among H_2-forming anaerobic bacteria.

The presence of H_2-sensing regulatory [FeFe]-hydrogenases (HydS) appears to be restricted to some H_2-forming anaerobic bacteria. In H_2-oxidizing aerobic bacteria, such as *Ralstonia eutropha*, and in H_2-oxidizing phototrophic bacteria, such as *Rhodobacter capsulatus*, H_2 is sensed by a regulatory [NiFe]-hydrogenase (HoxCB) in complex with the PAS domain-containing histidine kinase HoxJ. In the absence of H_2, HoxJ transfers phosphate to the transcriptional response regulator HoxA, which is inactive in the phosphorylated form. Biochemical and genetic data suggest that signal transduction between the regulatory [NiFe]-hydrogenase and HoxJ involves an electron transport process (80–86). The regulatory [NiFe]-hydrogenase contains an active site similar to that of the standard [NiFe]-hydrogenases. However, these enzymes

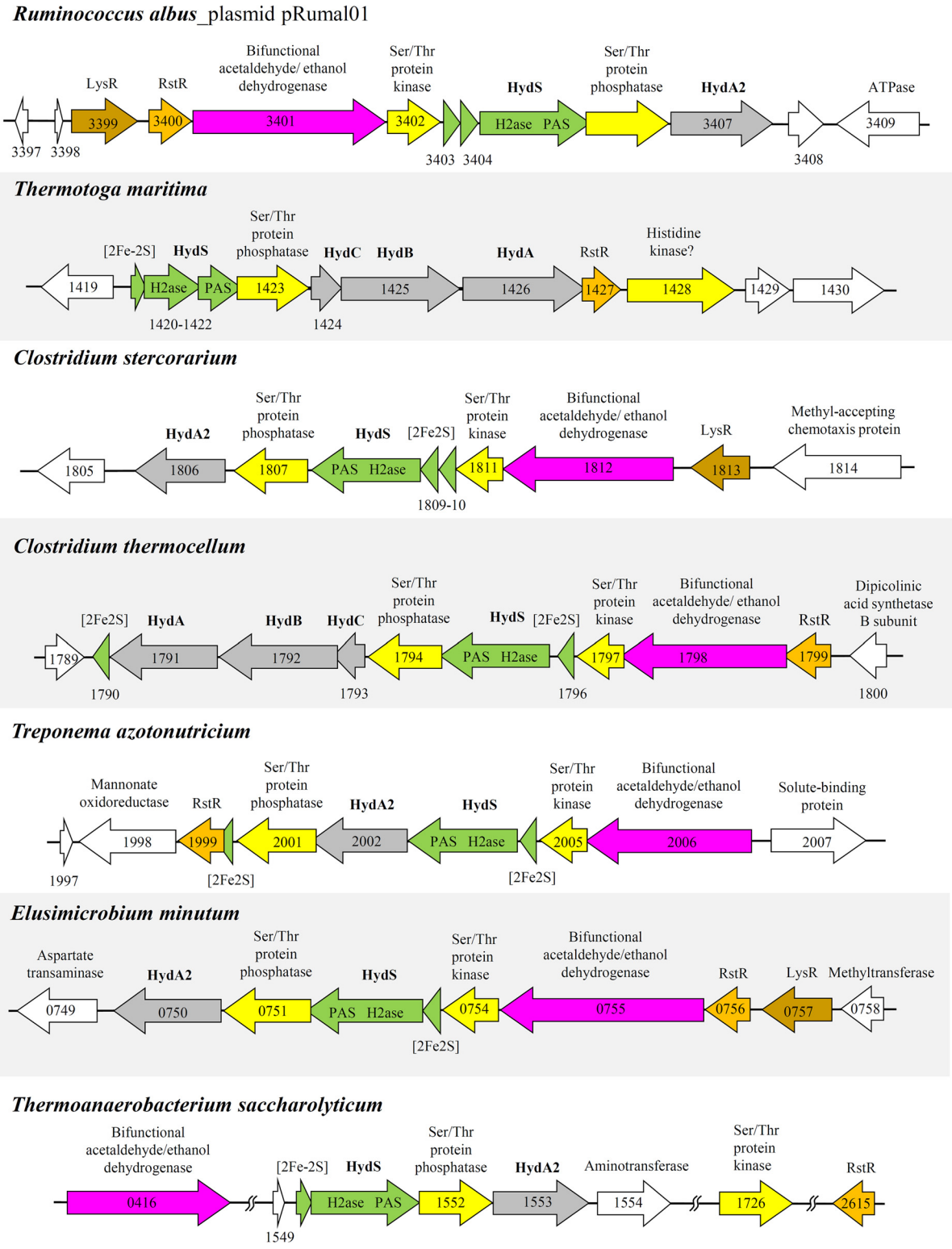

FIG 7 Genome region surrounding the gene encoding the putative H_2-sensing [FeFe]-hydrogenase HydS in seven representative bacteria. Rst, redox-sensing transcriptional repressor Rex; LysR, transcriptional regulator; HydA2, ferredoxin-dependent [FeFe]-hydrogenase; HydABC, electron-bifurcating ferredoxin- and NAD-dependent [FeFe]-hydrogenase. The numbers in the arrows correspond to genomic ORF identification numbers. HydS from *R. albus* 7 has 32% sequence similarity to HydS from *T. maritima*, 70% to HydS from *C. stercorarium*, 52% to HydS from *C. thermocellum*, 53% to HydS from *T. azotonutricium*, 63% to HydS from *E. minutum*, and 38% to HydS from *T. saccharolyticum*. HydA from *R. albus* 7 has 39% sequence similarity to HydA from *T. maritima*, 59% to HydA from *C. stercorarium*, 44% to HydA from *C. thermocellum*, 44% to HydA from *T. azotonutricium*, 44% to HydA from *E. minutum*, and 52% to HydA from *T. saccharolyticum*. HydA2 from *R. albus* 7 has 31% sequence similarity to HydA2 from *T. maritima*, 75% to HydA2 from *C. stercorarium*, 33% to HydA2 from *C. thermocellum*, 36% to HydA2 from *T. azotonutricium*, 70% to HydA2 from *E. minutum*, and 50% to HydA2 from *T. saccharolyticum*.

exhibit extremely low levels of activity, approximately 100-fold lower than those of the metabolic [NiFe]-hydrogenases (28). Thus, the mechanism of H_2 sensing via the regulatory [NiFe]-hydrogenase (HoxCB) may serve as a model for the elucidation of the mechanism of H_2 sensing via the regulatory [FeFe]-hydrogenase (HydS).

ACKNOWLEDGMENTS

This work was supported by the Max Planck Society and the Fonds der Chemischen Industrie.

REFERENCES

1. **Salonen A, de Vos WM.** 2014. Impact of diet on human intestinal microbiota and health. Annu. Rev. Food Sci. Technol. **5:**239–262. http://dx.doi.org/10.1146/annurev-food-030212-182554.
2. **Arumugam M, Raes J, Pelletier E, Le Paslier D, Yamada T, Mende DR, Fernandes GR, Tap J, Bruls T, Batto JM, Bertalan M, Borruel N, Casellas F, Fernandez L, Gautier L, Hansen T, Hattori M, Hayashi T, Kleerebezem M, Kurokawa K, Leclerc M, Levenez F, Manichanh C, Nielsen HB, Nielsen T, Pons N, Poulain J, Qin J, Sicheritz-Ponten T, Tims S, Torrents D, Ugarte E, Zoetendal EG, Wang J, Guarner F, Pedersen O, de Vos WM, Brunak S, Doré J, MetaHIT Consortium, Weissenbach J, Ehrlich SD, Bork P.** 2011. Enterotypes of the human gut microbiome. Nature **473:**174–180. http://dx.doi.org/10.1038/nature09944.
3. **Russell JB, Muck RE, Weimer PJ.** 2009. Quantitative analysis of cellulose degradation and growth of cellulolytic bacteria in the rumen. FEMS Microbiol. Ecol. **67:**183–197. http://dx.doi.org/10.1111/j.1574-6941.2008.00633.x.
4. **Morrison M, Pope PB, Denman SE, McSweeney CS.** 2009. Plant biomass degradation by gut microbiomes: more of the same or something new? Curr. Opin. Biotech. **20:**358–363. http://dx.doi.org/10.1016/j.copbio.2009.05.004.
5. **Moon YH, Iakiviak M, Bauer S, Mackie RI, Cann IKO.** 2011. Biochemical analyses of multiple endoxylanases from the rumen bacterium *Ruminococcus albus* 8 and their synergistic activities with accessory hemicellulose-degrading enzymes. Appl. Environ. Microbiol. **77:**5157–5169. http://dx.doi.org/10.1128/AEM.00353-11.
6. **Miron J, Ben-Ghedalla D, Morrison M.** 2001. Adhesion mechanisms of rumen cellulolytic bacteria. J. Dairy. Sci. **84:**1294–1309. http://dx.doi.org/10.3168/jds.S0022-0302(01)70159-2.
7. **Hungate RE.** 1957. Microorganisms in the rumen of cattle fed a constant ration. Can. J. Microbiol. **3:**289–311. http://dx.doi.org/10.1139/m57-034.
8. **Krause DO, Nagaraja TG, Wright ADG, Callaway TR.** 2013. Rumen microbiology: leading the way in microbial ecology. J. Anim. Sci. **91:**331–341. http://dx.doi.org/10.2527/jas.2012-5567.
9. **Hungate RE.** 1966. The rumen and its microbes. Academic Press, New York, NY.
10. **Hungate RE.** 1975. Rumen microbial ecosystem. Annu. Rev. Ecol. Syst. **6:**39–66. http://dx.doi.org/10.1146/annurev.es.06.110175.000351.
11. **Hungate RE.** 1967. Hydrogen as an intermediate in rumen fermentation. Arch. Mikrobiol. **59:**158–164. http://dx.doi.org/10.1007/BF00406327.
12. **Iannotti EL, Kafkewitz D, Wolin MJ, Bryant MP.** 1973. Glucose fermentation products of *Ruminococcus albus* grown in continuous culture with *Vibrio succinogenes*: changes caused by interspecies transfer of H_2. J. Bacteriol. **114:**1231–1240.
13. **Thauer RK, Jungermann K, Decker K.** 1977. Energy conservation in chemotropic anaerobic bacteria. Bacteriol. Rev. **41:**100–180.
14. **Ntaikou I, Gavala HN, Lyberatos G.** 2009. Modeling of fermentative hydrogen production from the bacterium *Ruminococcus albus*: definition of metabolism and kinetics during growth on glucose. Int. J. Hydrogen Energ. **34:**3697–3709. http://dx.doi.org/10.1016/j.ijhydene.2009.02.057.
15. **Stams AJM, Plugge CM.** 2009. Electron transfer in syntrophic communities of anaerobic bacteria and archaea. Nat. Rev. Microbiol. **7:**568–577. http://dx.doi.org/10.1038/nrmicro2166.
16. **Tewes FJ, Thauer RK.** 1980. Regulation of ATP-synthesis in glucose fermenting bacteria involved in interspecies hydrogen transfer, p 97–104. *In* Gottschalk G, Pfennig N, Werner H (ed), Anaerobes and anaerobic infections, G. Fischer Verlag, Stuttgart, Germany.
17. **Bennett BD, Kimball EH, Gao M, Osterhout R, Van Dien SJ, Rabinowitz JD.** 2009. Absolute metabolite concentrations and implied enzyme active site occupancy in *Escherichia coli*. Nat. Chem. Biol. **5:**593–599. http://dx.doi.org/10.1038/nchembio.186.
18. **Glass TL, Bryant MP, Wolin MJ.** 1977. Partial purification of ferredoxin from *Ruminococcus albus* and its role in pyruvate metabolism and reduction of nicotinamide adenine dinucleotide by H_2. J. Bacteriol. **131:**463–472.
19. **Tewes FJ, Thauer RK.** 1979. Purification and properties of ferredoxin from *Ruminococcus albus*. FEMS Microbiol. Lett. **6:**375–377. http://dx.doi.org/10.1111/j.1574-6968.1979.tb03746.x.
20. **Thauer RK, Kaster AK, Seedorf H, Buckel W, Hedderich R.** 2008. Methanogenic archaea: ecologically relevant differences in energy conservation. Nat. Rev. Microbiol. **6:**579–591. http://dx.doi.org/10.1038/nrmicro1931.
21. **Schut GJ, Adams MWW.** 2009. The iron-hydrogenase of *Thermotoga maritima* utilizes ferredoxin and NADH synergistically: a new perspective on anaerobic hydrogen production. J. Bacteriol. **191:**4451–4457. http://dx.doi.org/10.1128/JB.01582-08.
22. **Buckel W, Thauer RK.** 2013. Energy conservation via electron bifurcating ferredoxin reduction and proton/Na^+ translocating ferredoxin oxidation. Biochim. Biophys. Acta **1827:**94–113. http://dx.doi.org/10.1016/j.bbabio.2012.07.002.
23. **Schuchmann K, Müller V.** 2012. A bacterial electron-bifurcating hydrogenase. J. Biol. Chem. **287:**31165–31171. http://dx.doi.org/10.1074/jbc.M112.395038.
24. **Huang H, Wang S, Moll J, Thauer RK.** 2012. Electron bifurcation involved in the energy metabolism of the acetogenic bacterium *Moorella thermoacetica* growing on glucose or H_2 plus CO_2. J. Bacteriol. **194:**3689–3699. http://dx.doi.org/10.1128/JB.00385-12.
25. **Wang S, Huang H, Kahnt J, Thauer RK.** 2013. A reversible electron-bifurcating ferredoxin- and NAD-dependent [FeFe]-hydrogenase (HydABC) in *Moorella thermoacetica*. J. Bacteriol. **195:**1267–1275. http://dx.doi.org/10.1128/JB.02158-12.
26. **Wang S, Huang H, Kahnt J, Mueller AP, Köpke M, Thauer RK.** 2013. NADP-specific electron-bifurcating [FeFe]-hydrogenase in a functional complex with formate dehydrogenase in *Clostridium autoethanogenum* grown on CO. J. Bacteriol. **195:**4373–4386. http://dx.doi.org/10.1128/JB.00678-13.
27. **Suen G, Stevenson DM, Bruce DC, Chertkov O, Copeland A, Cheng JF, Detter C, Detter JC, Goodwin LA, Han CS, Hauser LJ, Ivanova NN, Kyrpides NC, Land ML, Lapidus A, Lucas S, Ovchinnikova G, Pitluck S, Tapia R, Woyke T, Boyum J, Mead D, Weimer PJ.** 2011. Complete genome of the cellulolytic ruminal bacterium *Ruminococcus albus* 7. J. Bacteriol. **193:**5574–5575. http://dx.doi.org/10.1128/JB.05621-11.
28. **Lubitz W, Ogata H, Rüdiger O, Reijerse E.** 2014. Hydrogenases. Chem. Rev. **114:**4081–4148. http://dx.doi.org/10.1021/cr4005814.
29. **Peters JW, Lanzilotta WN, Lemon BJ, Seefeldt LC.** 1998. X-ray crystal structure of the Fe-only hydrogenase (Cpl) from *Clostridium pasteurianum* to 1.8 angstrom resolution. Science **282:**1853–1858. http://dx.doi.org/10.1126/science.282.5395.1853.
30. **Henry JT, Crosson S.** 2011. Ligand-binding PAS domains in a genomic, cellular, and structural context. Annu. Rev. Microbiol. **65:**261–286. http://dx.doi.org/10.1146/annurev-micro-121809-151631.
31. **Wu M, Ren Q, Durkin AS, Daugherty SC, Brinkac LM, Dodson RJ, Madupu R, Sullivan SA, Kolonay JF, Haft DH, Nelson WC, Tallon LJ, Jones KM, Ulrich LE, Gonzalez JM, Zhulin IB, Robb FT, Eisen JA.** 2005. Life in hot carbon monoxide: the complete genome sequence of *Carboxydothermus hydrogenoformans* Z-2901. PLoS Genet. **1:**563–574. http://dx.doi.org/10.1371/journal.pgen.0010065.
32. **Mavromatis K, Ivanova N, Anderson I, Lykidis A, Hooper SD, Sun H, Kunin V, Lapidus A, Hugenholtz P, Patel B, Kyrpides NC.** 2009. Genome analysis of the anaerobic thermohalophilic bacterium *Halothermothrix orenii*. PLoS One **4:**e4192. http://dx.doi.org/10.1371/journal.pone.0004192.
33. **Ballor NR, Paulsen I, Leadbetter JR.** 2012. Genomic analysis reveals multiple [FeFe] hydrogenases and hydrogen sensors encoded by *Treponemes* from the H_2-rich termite gut. Microb. Ecol. **63:**282–294. http://dx.doi.org/10.1007/s00248-011-9922-8.
34. **Shaw AJ, Jenney FE, Adams MWW, Lynd LR.** 2008. End-product pathways in the xylose fermenting bacterium, *Thermoanaerobacterium saccharolyticum*. Enzyme Microb. Technol. **42:**453–458. http://dx.doi.org/10.1016/j.enzmictec.2008.01.005.
35. **Shaw AJ, Hogsett DA, Lynd LR.** 2009. Identification of the [FeFe]-hydrogenase responsible for hydrogen generation in *Thermoanaerobacte-*

rium saccharolyticum and demonstration of increased ethanol yield via hydrogenase knockout. J. Bacteriol. **191:**6457–6464. http://dx.doi.org/10.1128/JB.00497-09.
36. **Uyeda K, Rabinowitz JC.** 1971. Pyruvate-ferredoxin oxidoreductase. III. Purification and properties of enzyme. J. Biol. Chem. **246:**3111–3119.
37. **Schönheit P, Wäscher C, Thauer RK.** 1978. A rapid procedure for purification of ferredoxin from Clostridia using polyethyleneimine. FEBS Lett. **89:**219–222. http://dx.doi.org/10.1016/0014-5793(78)80221-X.
38. **Diekert GB, Graf EG, Thauer RK.** 1979. Nickel requirement for carbon monoxide dehydrogenase formation in *Clostridium pasteurianum*. Arch. Microbiol. **122:**117–120. http://dx.doi.org/10.1007/BF00408054.
39. **Theorell H, Bonnichsen R.** 1951. Studies on liver alcohol dehydrogenase. I. Equilibria and initial reaction velocities. Acta Chem. Scand. **5:**1105–1126.
40. **Wang S, Huang H, Moll J, Thauer RK.** 2010. $NADP^+$ reduction with reduced ferredoxin and $NADP^+$ reduction with NADH are coupled via an electron-bifurcating enzyme complex in *Clostridium kluyveri*. J. Bacteriol. **192:**5115–5123. http://dx.doi.org/10.1128/JB.00612-10.
41. **Watanabe T, Honda K.** 1982. Measurement of the extinction coefficient of the methyl viologen cation radical and the efficiency of its formation by semiconductor photocatalysis. J. Phys. Chem. **86:**2617–2619. http://dx.doi.org/10.1021/j100211a014.
42. **Michaelis L, Hill ES.** 1933. The viologen indicators. J. Gen. Physiol. **16:**859–873. http://dx.doi.org/10.1085/jgp.16.6.859.
43. **Lassak K, Neiner T, Ghosh A, Klingl A, Wirth R, Albers SV.** 2012. Molecular analysis of the crenarchaeal flagellum. Mol. Microbiol. **83:**110–124. http://dx.doi.org/10.1111/j.1365-2958.2011.07916.x.
44. **Miller TL, Wolin MJ.** 1973. Formation of hydrogen and formate by *Ruminococcus albus*. J. Bacteriol. **116:**836–846.
45. **Habenicht A.** 1997. The non-phosphorylating glyceraldehyde-3-phosphate dehydrogenase: biochemistry, structure, occurrence and evolution. Biol. Chem. **378:**1413–1419.
46. **Ito F, Chishiki H, Fushinobu S, Wakagi T.** 2012. Comparative analysis of two glyceraldehyde-3-phosphate dehydrogenases from a thermoacidophilic archaeon, *Sulfolobus tokodaii*. FEBS Lett. **586:**3097–3103. http://dx.doi.org/10.1016/j.febslet.2012.07.059.
47. **Park MO, Mizutani T, Jones PR.** 2007. Glyceraldehyde-3-phosphate ferredoxin oxidoreductase from *Methanococcus maripaludis*. J. Bacteriol. **189:**7281–7289. http://dx.doi.org/10.1128/JB.00828-07.
48. **Mukund S, Adams MWW.** 1995. Glyceraldehyde-3-phosphate ferredoxin oxidoreductase, a novel tungsten-containing enzyme with a potential glycolytic role in the hyperthermophilic archaeon *Pyrococcus furiosus*. J. Biol. Chem. **270:**8389–8392. http://dx.doi.org/10.1074/jbc.270.15.8389.
49. **Debnar-Daumler C, Seubert A, Schmitt G, Heider J.** 2014. Simultaneous involvement of a tungsten-containing aldehyde: ferredoxin oxidoreductase and a phenylacetaldehyde dehydrogenase in anaerobic phenylalanine metabolism. J. Bacteriol. **196:**483–492. http://dx.doi.org/10.1128/JB.00980-13.
50. **Extance J, Crennell SJ, Eley K, Cripps R, Hough DW, Danson MJ.** 2013. Structure of a bifunctional alcohol dehydrogenase involved in bioethanol generation in *Geobacillus thermoglucosidasius*. Acta Crystallogr. D Biol. Crystallogr. **69:**2104–2115. http://dx.doi.org/10.1107/S0907444913020349.
51. **Aboulnaga EH, Pinkenburg O, Schiffels J, El-Refai A, Buckel W, Selmer T.** 2013. Butyrate production in *Escherichia coli*: exploitation of an oxygen tolerant bifurcating butyryl-CoA dehydrogenase/electron transferring flavoprotein complex from *Clostridium difficile*. J. Bacteriol. **195:**3704–3713. http://dx.doi.org/10.1128/JB.00321-13.
52. **Li F, Hinderberger J, Seedorf H, Zhang J, Buckel W, Thauer RK.** 2008. Coupled ferredoxin and crotonyl coenzyme A (CoA) reduction with NADH catalyzed by the butyryl-CoA dehydrogenase/Etf complex from *Clostridium kluyveri*. J. Bacteriol. **190:**843–850. http://dx.doi.org/10.1128/JB.01417-07.
53. **Weghoff MC, Bertsch J, Müller V.** 2014. A novel mode of lactate metabolism in strictly anaerobic bacteria. Environ. Microbiol. http://dx.doi.org/10.1111/1462-2920.12493.
54. **Bertsch J, Parthasarathy A, Buckel W, Müller V.** 2013. An electron-bifurcating caffeyl-CoA reductase. J. Biol. Chem. **288:**11304–11311. http://dx.doi.org/10.1074/jbc.M112.444919.
55. **Hess V, Schuchmann K, Müller V.** 2013. The ferredoxin:NAD^+ oxidoreductase (Rnf) from the acetogen *Acetobacterium woodii* requires Na^+ and is reversibly coupled to the membrane potential. J. Biol. Chem. **288:**31496–31502. http://dx.doi.org/10.1074/jbc.M113.510255.
56. **Alves L, Cyrne L, Amaral-Collaco MT, Girio FM.** 2003. Evidence of aerobic and anaerobic format dehydrogenase and aldehyde dehydrogenase immunological similarities shown by polyclonal antibodies raised against molybdoproteins. World J. Microb. Biot. **19:**201–208. http://dx.doi.org/10.1023/A:1023242032407.
57. **Ragsdale SW, Pierce E.** 2008. Acetogenesis and the Wood-Ljungdahl pathway of CO_2 fixation. Biochim. Biophys. Acta **1784:**1873–1898. http://dx.doi.org/10.1016/j.bbapap.2008.08.012.
58. **Shanmugasundaram T, Wood HG.** 1992. Interaction of ferredoxin with carbon monoxide dehydrogenase from *Clostridium thermoaceticum* J. Biol. Chem. **267:**897–900.
59. **Thauer RK, Kaster AK, Goenrich M, Schick M, Hiromoto T, Shima S.** 2010. Hydrogenases from methanogenic archaea, nickel, a novel cofactor, and H_2 storage. Annu. Rev. Biochem. **79:**507–536. http://dx.doi.org/10.1146/annurev.biochem.030508.152103.
60. **Burnside K, Rajagopal L.** 2012. Regulation of prokaryotic gene expression by eukaryotic-like enzymes. Curr. Opin. Microbiol. **15:**125–131. http://dx.doi.org/10.1016/j.mib.2011.12.006.
61. **Pereira SFF, Goss L, Dworkin J.** 2011. Eukaryote-like serine/threonine kinases and phosphatases in bacteria. Microbiol. Mol. Biol. R. **75:**192–212. http://dx.doi.org/10.1128/MMBR.00042-10.
62. **Solovyev V, Salamov A.** 2011. Automatic annotation of microbial genomes and metagenomic sequences, p 61–78. *In* Li RW (ed), Metagenomics and its applications in agriculture, biomedicine and environmental studies. Nova Science Publishers, New York, NY.
63. **Hofacker IL, Fontana W, Stadler PF, Bonhoeffer LS, Tacker M, Schuster P.** 1994. Fast folding and comparison of RNA secondary structures. Monash. Chem. **125:**167–188. http://dx.doi.org/10.1007/BF00818163.
64. **Macke TJ, Ecker DJ, Gutell RR, Gautheret D, Case DA, Sampath R.** 2001. RNAMotif, an RNA secondary structure definition and search algorithm. Nucleic Acids Res. **29:**4724–4735. http://dx.doi.org/10.1093/nar/29.22.4724.
65. **Lesnik EA, Sampath R, Levene HB, Henderson TJ, McNeil JA, Ecker DJ.** 2001. Prediction of rho-independent transcriptional terminators in *Escherichia coli*. Nucleic Acids Res. **29:**3583–3594. http://dx.doi.org/10.1093/nar/29.17.3583.
66. **Gautheret D, Lambert A.** 2001. Direct RNA motif definition and identification from multiple sequence alignments using secondary structure profiles. J. Mol. Biol. **313:**1003–1011. http://dx.doi.org/10.1006/jmbi.2001.5102.
67. **Maddocks SE, Oyston PCF.** 2008. Structure and function of the LysR-type transcriptional regulator (LTTR) family proteins. Microbiology **154:**3609–3623. http://dx.doi.org/10.1099/mic.0.2008/022772-0.
68. **Ogura T, Wilkinson AJ.** 2001. AAA(+) superfamily ATPases: common structure-diverse function. Genes Cells **6:**575–597. http://dx.doi.org/10.1046/j.1365-2443.2001.00447.x.
69. **Mutalik S, Kumar CSV, Swamy S, Manjappa S.** 2012. Hydrolysis of lignocellulosic feed stock by *Ruminococcus albus* in production of biofuel ethanol. Ind. J. Biotechnol. **11:**453–457.
70. **Wang E, Ikonen TP, Knaapila M, Svergun D, Logan DT, von Wachenfeld C.** 2011. Small-angle X-ray scattering study of a Rex family repressor: conformational response to NADH and NAD^+ binding in solution. J. Mol. Biol. **408:**670–683. http://dx.doi.org/10.1016/j.jmb.2011.02.050.
71. **Sickmier EA, Brekasis D, Paranawithana S, Bonanno JB, Paget MSB, Burley SK, Kielkopf CL.** 2005. X-ray structure of a Rex-family repressor/NADH complex insights into the mechanism of redox sensing. Structure **13:**43–54. http://dx.doi.org/10.1016/j.str.2004.10.012.
72. **Gyan S, Shiohira Y, Sato I, Takeuchi M, Sato T.** 2006. Regulatory loop between redox sensing of the NADH/NAD^+ ratio by Rex (YdiH) and oxidation of NADH by NADH dehydrogenase Ndh in *Bacillus subtilis*. J. Bacteriol. **188:**7062–7071. http://dx.doi.org/10.1128/JB.00601-06.
73. **McLaughlin KJ, Strain-Damere CM, Xie K, Brekasis D, Soares AS, Paget MSB, Kielkopf CL.** 2010. Structural basis for NADH/NAD^+ redox sensing by a Rex family repressor. Mol. Cell **38:**563–575. http://dx.doi.org/10.1016/j.molcel.2010.05.006.
74. **Bielen AAM, Verhaart MRA, VanFossen AL, Blumer-Schuette SE, Stams AJM, van der Oost J, Kelly RM, Kengen SWM.** 2013. A thermophile under pressure: transcriptional analysis of the response of *Caldicellulosiruptor saccharolyticus* to different H_2 partial pressures. Int. J. Hydrogen Energ. **38:**1837–1849. http://dx.doi.org/10.1016/j.ijhydene.2012.11.082.

75. **Kennelly PJ.** 2014. Protein Ser/Thr/Tyr phosphorylation in the archaea. J. Biol. Chem. **289:**9480–9487. http://dx.doi.org/10.1074/jbc.R113.529412.
76. **Nelson KE, Clayton RA, Gill SR, Gwinn ML, Dodson RJ, Haft DH, Hickey EK, Peterson LD, Nelson WC, Ketchum KA, McDonald L, Utterback TR, Malek JA, Linher KD, Garrett MM, Stewart AM, Cotton MD, Pratt MS, Phillips CA, Richardson D, Heidelberg J, Sutton GG, Fleischmann RD, Eisen JA, White O, Salzberg SL, Smith HO, Venter JC, Fraser CM.** 1999. Evidence for lateral gene transfer between Archaea and Bacteria from genome sequence of *Thermotoga maritima*. Nature **399:** 323–329. http://dx.doi.org/10.1038/20601.
77. **Poehlein A, Zverlov VV, Daniel R, Schwarz WH, Liebl W.** 2013. Complete genome sequence of *Clostridium stercorarium* subsp. stercorarium strain DSM 8532, a thermophilic degrader of plant cell wall fibers. Genome Announc. **1:**e0007313. http://dx.doi.org/10.1128/genomeA.00073-13.
78. **Feinberg L, Foden J, Barrett T, Davenport KW, Bruce D, Detter C, Tapia R, Han C, Lapidus A, Lucas S, Cheng JF, Pitluck S, Woyke T, Ivanova N, Mikhailova N, Land M, Hauser L, Argyros DA, Goodwin L, Hogsett D, Caiazza N.** 2011. Complete genome sequence of the cellulolytic thermophile *Clostridium thermocellum* DSM1313. J. Bacteriol. **193:** 2906–2907. http://dx.doi.org/10.1128/JB.00322-11.
79. **Herlemann DPR, Geissinger O, Ikeda-Ohtsubo W, Kunin V, Sun H, Lapidus A, Hugenholtz P, Brune A.** 2009. Genomic analysis of "*Elusimicrobium minutum*," the first cultivated representative of the phylum "*Elusimicrobia*" (formerly termite group 1). Appl. Environ. Microbiol. **75:**2841–2849. http://dx.doi.org/10.1128/AEM.02698-08.
80. **Vignais PM.** 2009. Regulation of hydrogenase gene expression, p 743–757. *In* Govindjee, Sharkey TD (ed), Advances in photosynthesis and respiration: including bioenergy and related processes. Springer, Dordrecht, Netherlands.
81. **Greening C, Cook GM.** 2014. Integration of hydrogenase expression and hydrogen sensing in bacterial cell physiology. Curr. Opin. Microbiol. **18:** 30–38. http://dx.doi.org/10.1016/j.mib.2014.02.001.
82. **Löscher S, Gebler A, Stein M, Sanganas O, Buhrke T, Zebger I, Dau H, Friedrich B, Lenz O, Haumann M.** 2010. Protein-protein complex formation affects the Ni-Fe and Fe-S centers in the H_2-sensing regulatory hydrogenase from *Ralstonia eutropha* H16. Chemphyschem **11:**1297–1306. http://dx.doi.org/10.1002/cphc.200901007.
83. **Buhrke T, Löscher S, Lenz O, Schlodder E, Zebger I, Andersen LK, Hildebrandt P, Meyer-Klaucke W, Dau H, Friedrich B, Haumann M.** 2005. Reduction of unusual iron-sulfur clusters in the H_2-sensing regulatory Ni-Fe hydrogenase from *Ralstonia eutropha* H16. J. Biol. Chem. **280:** 19488–19495. http://dx.doi.org/10.1074/jbc.M500601200.
84. **Buhrke T, Lenz O, Porthun A, Friedrich B.** 2004. The H_2-sensing complex of *Ralstonia eutropha*: interaction between a regulatory [NiFe] hydrogenase and a histidine protein kinase. Mol. Microbiol. **51:**1677–1689. http://dx.doi.org/10.1111/j.1365-2958.2003.03933.x.
85. **Elsen S, Duché O, Colbeau A.** 2003. Interaction between the H_2 sensor HupUV and the histidine kinase HupT controls HupSL hydrogenase synthesis in *Rhodobacter capsulatus*. J. Bacteriol. **185:**7111–7119. http://dx.doi.org/10.1128/JB.185.24.7111-7119.2003.
86. **Lenz O, Bernhard M, Buhrke T, Schwartz E, Friedrich B.** 2002. The hydrogen-sensing apparatus in *Ralstonia eutropha*. J. Mol. Microbiol. Biotechnol. **4:**255–262.
87. **Smith ET, Bennett DW, Feinberg BA.** 1991. Redox properties of 2[4fe-4s] ferredoxins. Anal. Chim. Acta **251:**27–33. http://dx.doi.org/10.1016/0003-2670(91)87111-J.